frontiers | Frontiers in Environmental Science

TYPE Original Research
PUBLISHED 21 September 2022
DOI 10.3389/fenvs.2022.981104

OPEN ACCESS

EDITED BY
Xiaolan Li,
Institute of Atmospheric Environment, CMA, China

REVIEWED BY
Ningwei Liu,
China Meteorological Administration, Shenyang, China
Shengzhen Zhou,
Sun Yat-Sen University, China

*CORRESPONDENCE
Jizhi Wang,
jzwang@cma.gov.cn

SPECIALTY SECTION
This article was submitted to Atmosphere and Climate, a section of the journal Frontiers in Environmental Science

RECEIVED 29 June 2022
ACCEPTED 16 August 2022
PUBLISHED 21 September 2022

CITATION
Wang D, Wang J, Yang Y, Jia W, Jiang X and Wang Y (2022), Impact of meteorological conditions on tropospheric ozone and associated with parameterization methods for quantitative assessment and monitoring.
Front. Environ. Sci. 10:981104.
doi: 10.3389/fenvs.2022.981104

Impact of meteorological conditions on tropospheric ozone and associated with parameterization methods for quantitative assessment and monitoring

Deying Wang[1], Jizhi Wang[1]*, Yuanqin Yang[1], Wenxing Jia[1], Xiaofei Jiang[2] and Yaqiang Wang[1]

[1]State Key Laboratory of Severe Weather and Key Laboratory of Atmospheric Chemistry of CMA, Chinese Academy of Meteorological Sciences, Beijing, China, [2]China Meteorological Administration Training Centre, Beijing, China

In recent years, the heavy ozone pollution events around the world have shown a sudden frequently increase, which has aroused widespread concern in the government and the public. It is well known that O_3 is driven by photochemical reactions triggered by solar radiation (direct and indirect solar radiation), the O_3 concentration calculated by chemical mechanism is mostly significantly lower than the actual O_3 observation. Based on the study of the effect of meteorological conditions on the "additional increment" of O_3 in three representative regions of Beijing, Hangzhou and Guangzhou from 2015 to 2020, an innovation diagnostic theory algorithm that the cross-cutting effects of atmospheric clouds on the chemical pattern of O_3 solar radiation is established in this study. On this basis, a parametric evaluation method of O_3 is established. The novelty of this study is 1) Comprehensive influence of the meteorological conditions and photochemical reactions mechanisms on the cross-cutting effects of O_3 concentration are given. Especially low-level clouds in the troposphere, which have significantly large variable effects on the reflection and refraction of O_3 through solar radiation. Theory quantitative algorithm of cloud scattering, cloud height, cloud volume and cloud structure changes, as well as feedback effects caused by water vapor condensation, which closely related to the transformation of O_3 precursors are given. 2) Based on this, a parameterization method for quantitative O_3 assessment and monitoring, which is a Parameterization for Linking Ozone pollution with Meteorological conditions. 3) Applying the theoretical algorithm and parameterization method of this study, comparing the changes of O_3 in 2018 with 2019, an objective quantitative distinction between emission reduction and meteorological impact was made, showing that emission reduction still played a leading role, with a contribution rate of about 27%. This shows that the created quantitative algorithm of atmospheric cloud theory and the innovative parameterization method can provide an objective

quantitative basis for O_3 pollution decision-making and public emission reduction.

KEYWORDS

meteorological conditions, parameterization method, solar zenith angle, cloud scattering, Ozone pollution

Highlights

·O_3 concentrations vary with cloud reflections driven by Θ_z diurnal variations.
·High condensation under high humidity in the air is conducive to a re-increase in O_3
·Parameterize for quantitative assessment of impact of meteorological conditions on O_3
·PLOM constructs application of O_3-value add theory based on multi-factor contribution

1 Introduction

In recent years, the tropospheric (or near-surface) O_3 concentration has significantly increased. High-resolution synchronous observation revealed that the O_3 concentration in the troposphere increased by −10%–40% when the nitrogen oxide concentration decreased to a certain level during the period of the Beijing 2008 Olympic Monitoring Campaign (Zhang et al., 2009). China suffered from O_3 pollution during several consecutive high-temperature weather periods during the summers of 2017–2020. From July 17 to 20 July 2017, O_3 pollution occurred in many places in the North China Plain (NCP), Northeast China, and Northwest China, with a particularly long period in Beijing, and the frequent occurrences of heavy O_3 pollution in recent years. The formation and control of O_3 have become important issues of concern to the government and public.

Although the impact of clouds and aerosols on climate has been studied for decades, it remains a complex and unsolved problem. The aerosol effect on enhancing cloud albedo, which is often called the first aerosol indirect effect. For climate patterns where uncertainties are mostly present, the impact of atmospheric clouds is important, because it is difficult to exclude the feedback of different surface fluxes on turbulence dynamics, including the impact of cloud characteristics on the O_3 concentrations, so the influence of meteorological conditions on atmospheric tropospheric O_3 concentrations needs to be carefully studied and diagnosed (Wang and McFarquhar, 2008). (Wang and McFarquhar 2008) Modeling aerosol effects on shallow cumulus convection under various meteorological conditions observed over the Indian Ocean and implications for development of mass-flux parameterizations for climate models.

The effects of cloud cover, cloud height and cloud amount on solar radiation are directly related. The cloud amount is defined as a percentage of the horizontal domain covered by the cloud column at any level. The cloud amount continues to increase as relative humidity (RH) increases. For example, in the clean environment, the mean cloud amount increased from 6% to 11%, when RH increases from 49% to 80%. This indicates that atmospheric clouds are closely related to humidity, condensation rate, and super-saturation. These complex atmospheric cloud problems affect the solar radiation and photochemical reaction mechanism of O_3.

It is well-known that O_3 is driven by photochemical reactions initiated by solar radiation (for sure including direct and indirect solar radiation). A steady-state concentration of O_3 is expressed as follows (Madronich and Flocke, 1999; Textor et al., 2006):

$$[O_3] = \frac{j[NO_2]}{k[NO]} \tag{1}$$

where j is the photolysis frequency of NO_2, k is the rate coefficient for the O_3+NO->NO_2+O_2 reaction and the brackets denote the concentrations of O_3, NO_2 and NO.

The above relationship of NO, NO_2, and O_3 is called a steady-state relationship. Its dynamic equation is also given as (Tang et al., 2006):

$$[O_3] = \left\{\left[\left(\frac{j}{k}\right)^2 + 4\frac{j}{k}[NO_2]_0\right]^{\frac{1}{2}} - \frac{j}{k}\right\} \tag{2}$$

where the basic photochemical cycle of NO_2, NO, and O_3 is the fundamental source for O_3 genesis; j and k are constants of transformation efficiency in chemical reactions. Then it also be expressed as $\alpha = \frac{j}{k} \approx 0.01 \times 10^{-6}$, as a coefficient for the transformation efficiency (Textor et al., 2006; Wang et al., 2019).

However, in most cases, calculations of the chemical mechanism given in expression (2), even including other expression, are often underestimated compared to actual O_3 observations (Textor et al., 2006; Wang et al., 2019). Studies suggest that it is because for use in photo-chemistry models, and routinely include the effects of molecular absorbers and scatterers, clouds, aerosols, and surface reflections. So that, for different location and time of the year. Actual atmospheric conditions needed as input to the calculation are often not available (Madronich and Flocke, 1999).

So that the changes in tropospheric meteorological conditions should be one of the important factors to consider. In particular, the O_3 generation mechanism based on photochemistry and optical radiation is closely related to structural changes in the tropospheric low-layer cloud field

and their variable influence on the reflection and refraction of solar radiation. As mentioned above, the O_3 chemical mechanism is an approximation. Values j depend on molecular parameters (absorption cross sections and photo-dissociation quantum yields) that are specific to the photo-reaction of interest, and on the availability of solar radiation at any specific location in the atmosphere (Tang et al., 2006).

The quantifying the impacts of unfavorable meteorological conditions on tropospheric O_3 variation is the key issue for the Meteorological Forecasting Center to accurately assess of O_3. Nor can O_3 pollution prevention and control be decoupled from meteorological impacts. Research on the severe O_3 pollution events in the mega cities of China (Hangzhou, Guangzhou, Chengdu, and Beijing) has shown that meteorological conditions play a critical role in such phenomena (Wang and Chai, 2002; Li et al., 2015; Hu et al., 2016; Wang et al., 2019). Wang et al. (2018) selected two stations in the inland and ocean near Hong Kong to simultaneously monitor the main and secondary pollutant (e.g., O_3, NO, NO_2, and SO_2) concentrations. The results demonstrate that the O_3 concentration adjacent to the offshore point was much higher than that at the land point, indicating that the entry of continental high-pressure air mass into the sea, the tropical cyclone activities, and the interaction of the land-sea breeze all contribute to O_3 changes (Wang et al., 2018). Although there is some progress in research on the influence of meteorological conditions on air quality, it is still in the analysis stage and there is a lack of objective quantitative model-based research on the possible impact of meteorological conditions on O_3 pollution (Zhang et al., 2011; Yang et al., 2015; Hu et al., 2016). In this study, we try to adopt the parametric method to introduce the effects of cloud scattering, temperature, humidity, atmospheric density and other changes under the condition of solar zenith angle change, and explore the additional value-added effect of meteorological conditions on O_3 concentration.

As mentioned above, in particular, the O_3 generation mechanism based on photochemistry and optical radiation is closely related to structural changes in the tropospheric low-layer cloud field and their variable influence on the reflection and refraction of solar radiation. As an important factor affecting troposphere O_3, the intensity of solar ultraviolet radiation, the atmospheric channel of sunlight, and especially the impact of near-surface atmospheric meteorological conditions is extremely important. When the solar zenith angle changes, the reflection path length of solar radiation passing through clouds with different structures will naturally change; this affects and changes the O_3 content in the atmosphere (Bohn et al., 2008). All characteristics of skies with or without clouds, such as cloud height, cloud shape, cloud amount, cloud thickness, and light transmittance, affect and change the radiation path length, and then influence solar radiation. Changes in the cloud and solar zenith angle superimpose and offer feedback to further update the temporal and spatial distribution and changes in O_3 concentration. Data and research on these aspects are lacking.

An increase in O_3 concentration is closely related to the interaction between solar radiation and cloud structure (Webb and Steven, 1986; Zhao et al., 2019). Continuous cloud cover and sunlight can be often observed when looking down from aircraft. After reflection and scattering, the sky brightness increases. The differences between the cloud structure and the density of upper and lower clouds are related to the interaction between the temperature (T), pressure (P), and relative humidity (RH). The direct and feedback effects of meteorological conditions change the photochemical radiation intensity to drive the proliferation or reduction of O_3 and then affect its temporal and spatial redistribution (Bokoye et al., 2001).

Based on the principle of the PLAM index of pollution-causing meteorological conditions (Yang et al., 2009; Zhang et al., 2009, 2013, 2018), this study further investigated the relationship between O_3 pollution and meteorological conditions by parameterization, focusing on the meteorological conditions in the sensitive areas with frequent high-concentration O_3 and high-concentration regions, including the NCP, Yangtze River Delta (YRD), and Pearl River Delta (PRD). Through the analysis of multi-regional temporal and spatial observational data, this study identified the meteorological conditions affecting O_3 pollution, including the contribution of cloud reflection and the correlation between the cloud structure and solar zenith angle. The objective method to describe the relationship between O_3 pollution and meteorological conditions was quantified.

2 Data and methods

2.1 Data used in the study

Atmospheric observation data of 2015–2020 for the city areas of Beijing, Hangzhou, and Guangzhou, the major pollution influence areas of China, were supplied by the China Meteorological Information Center. Real-time and historical data of surrounding areas, including air temperature, dew temperature, air pressure, wind direction, wind speed, and visibility, were obtained from the observation stations and Hour Resolution of Automatic Weather Station (AWS) and the re-analysis data of the China Climate Center Figure Forecasting System for 2015–2020.

The geographical distribution of the NCP, YRD, and PRD regions, represented by Beijing, Hangzhou, Guangzhou, and other cities, is shown in Figure 1. The analytical data on condensation rate (f_c), wet potential temperature (θ_e), and super-saturation (S) were obtained from previous studies (Zhang et al., 2009; Wang et al., 2017; Liu et al., 2019; Wang et al., 2021). The atmospheric composition data, including $PM_{2.5}$, O_3, NO_2, SO_2, and PM_{10} over Beijing, Hangzhou, and Guangzhou in 2015–2020, were obtained from the Ministry of Ecology and Environment (http://www.zhb.gov.cn/hjzl/).

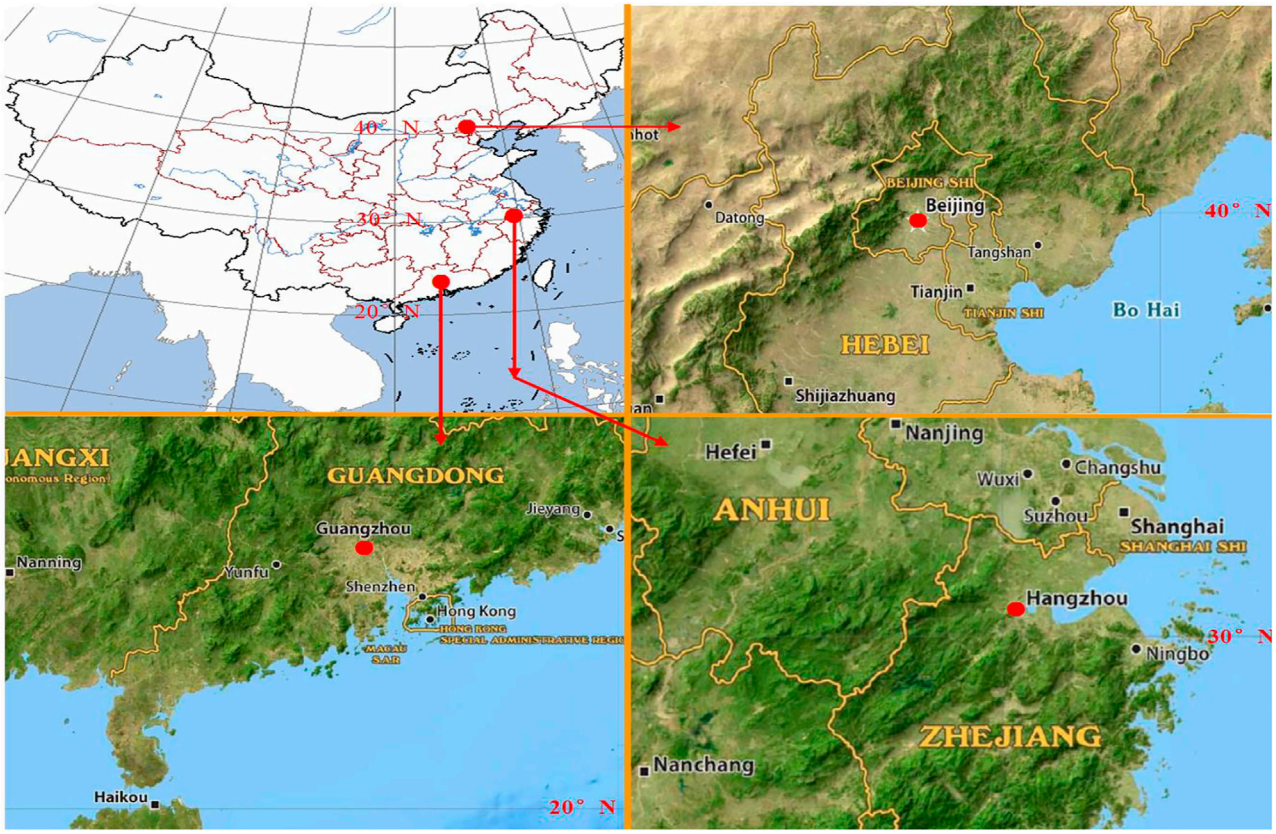

FIGURE 1
The geographical distribution of the North China Plain (NCP), Yangtze River Delta (YRD) and Pearl River Delta (PRD) regions represented by Beijing, Hangzhou, Guangzhou and other cities.

2.2 Methods

Because the levels of air pollutants, including O_3, are generally controlled by a combination of multi-meteorological variables, the impacts of individual meteorological variables on air pollution may not be significant and/or may cancel each other, as they can hardly account for the interrelation between the variables (Li et al., 2011; Wang et al., 2012). In this study, multi-sensitivity meteorological parameters were analyzed with regard to the influence of cloud scattering, solar heating, and other factors on the mechanism of O_3 changes. The new developing of the methods in this study are as follows:

2.2.1 The development of parameterization method

At present, the understanding of some atmospheric microphysical or atmospheric chemical processes related to air quality growth is not very clear and needs to be further explored. Some physical equations are inherently uncertain, or the necessary observational information under current conditions is unknown or difficult to measure precisely. For example, the physical processes of atmospheric clouds are closely related to the increase of O_3 concentration, the convection of cumulus clouds in the atmosphere, and the instantaneous mixing and change of temperature in the cloud and the ambient temperature. These processes are often difficult to write deterministic equations. Guo H-L's famous series of studies on parameterization (Kuo, 1961; Kuo, 1965; Kuo, 1974) pioneered the use of cloud microphysical processes and large-scale observational information as parametric schemes, which are widely used in numerical weather prediction. The results of the research show that the parametric method links the so-called "different magnitudes" and "incomparable" atmospheric micro-scale physical processes with large-scale processes. By parameterize and making connections between some sensitivity factors, the solution of the physical equations can be obtained.

2.2.2 The parameterization method

A parameterization method, that The Parameterization to Link Ozone-pollution with Meteorological conditions (PLOM) is mainly focused on the following sensitive influencing factors: 1) changes of solar zenith angle (Θ_z) in local time; 2) variation in and formation of

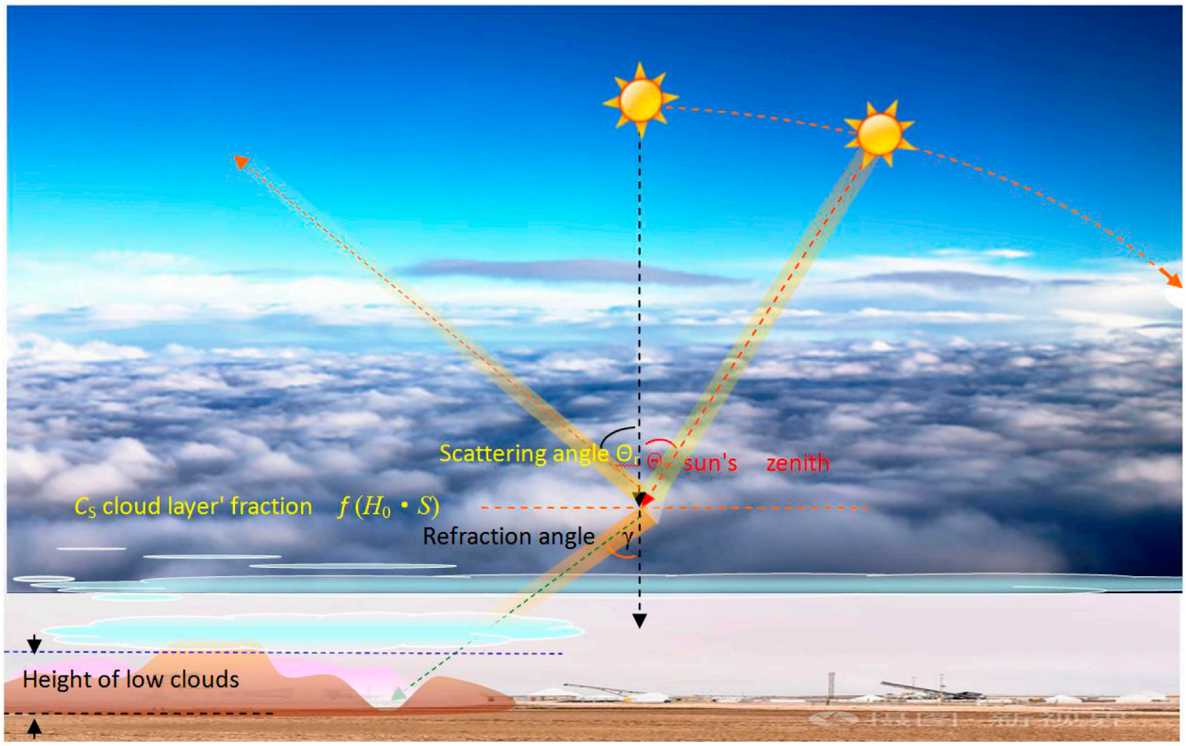

FIGURE 2
Physical model of the relationship between the reflection, refraction of solar and solar zenith angle by atmospheric clouds.

cloud scattering angle (Θ_r), and contribution of cloud scattering changes (Γ_Θ); 3) cloud structure (H_0), including cloud height, cloud amount, and cloud shape; and 4) contribution of water vapor condensation and humidification of precursor emissions to increases in O_3 concentration (ξ). The basic factors closely related to the parameterization include the atmospheric condensation rate (f_c), temperature (T), pressure (P), and atmospheric density variation (ρ).

2.2.3 Contribution of solar zenith angle parameter (Θ_z) and cloud scattering (Γ_Θ) to O_3 concentration

The contributions of the solar zenith angle parameter (Θ_z) and cloud scattering (Γ_Θ) are inseparable. Figure 2 presents a schematic diagram of the relationship between solar scattering/reflection, refraction, solar zenith angle, and atmospheric clouds. The results show that the solar reflection (diffuse reflection) rule is also applicable to scattering (Webb and Steven, 1986; Zhao et al., 2019). The solar zenith angle (Θ_z) is the angle between the incident light and the normal on the ground.

Γ_Θ is the O_3 comprehensive influence parameter under the effects of meteorological conditions and different solar zenith angles; it describes the impacts of clouds on reflection, refraction, and scattering. The reflections of sunlight by fog and cloud, and the variation in the reflection angle between air masses with different densities depend on the changes in the vertical gradient of the atmospheric pressure (P), temperature (T), and relative humidity (RH) (Zhao et al., 2019). These changes will also depend on the vertical difference in atmospheric density (ρ). They are expressed using the classical theory of atmospheric optics (Humphreys, 1940):

$$\Theta_r = \sin^{-1}\left(\frac{\rho'}{\rho}\right)^{1/2} \tag{3}$$

Where $\rho = \frac{P}{R_d T_v}$ represents the comprehensive influence of pressure (P), temperature (T), and virtual temperature [T_v, $T_v = (1 + 0.61w)$]; w is the humidity parameter mixing ratio; and $R_d = 2.8705 \times 10^{-1}$ J $g^{-1}°C^{-1}$ is the gas constant. Considering the air density difference above and below the cloud, the cloud scattering angle replaces the zenith angle under the condition of clear skies and no clouds. For a certain zenith angle during the day, the contribution of cloud scattering to the increment in O_3 concentration is:

$$\Gamma_\Theta = \mu \cos \Theta_z \begin{cases} \Theta_z = \Theta_\gamma = \sin^{-1}\left(\frac{\rho'}{\rho}\right)^{1/2} \text{considering the density difference above and below clouds} \\ \Theta_z \text{when there are no clouds and the density difference of the air layer is zero.} \end{cases} \tag{4}$$

Where μ - single scattering albedo, the efficiency coefficient associated with cloud structure (Sheng et al., 2019). Scattering albedo (μ) is related to the cloud height (H_0) of the reflected clouds, the cloud layer is higher, the scattering rate of light is higher, take 0.9–1.5. Conversely, the cloud layer is lower, the scattering rate of light is lower, generally fluctuating between 0.75 and 0.85.

As shown in Figure 2, solar radiation is reflected and scattered due to the atmospheric density difference above and below the cloud, resulting in a change in the scattering angle. γ is the refraction angle of solar radiation below the cloud in Figure 2.

Eq. 3 implies that when solar radiation encounters the influential cloud layer before reaching the ground, the density difference between the cloud and the regions above and below the cloud shall be considered; the relationship expression of Γ_Θ is $\Gamma_\Theta = \mu\cos\Theta_\gamma = \mu\cos(\sin^{-1}(\frac{\rho'}{\rho})^{1/2})$. When there are no clouds and the density difference of the atmospheric layer is zero, $\Gamma_\Theta = \mu\cos\Theta_z$.

2.2.4 Atmospheric cloud height

Atmospheric cloud structure is one of the important meteorological parameters that affect O_3 concentration; clouds play an important role in the energy balance of the earth system. The structural differences in cloud height, shape, and amount have a significant impact on the heating or cooling of different atmospheric stratifications. When clouds reflect sunlight back into space, the level above the clouds gets heated, whereas absorption of solar radiation by clouds results in cooling of the atmosphere below them. In the climate model, one of the sources of inaccuracy in prediction is the uncertainty in the description of the impact of cloud structure in the climate system, including the reflection of clouds, which is an important meteorological parameter that affects O_3 concentration (Platnick et al., 2000; Qu and Chen, 2002; Ackerman et al., 2004; Dunya et al., 2017). Under conditions that systematically affect clouds, the cloud height (H_0) is a fundamental parameter of atmospheric clouds. Solar radiation is influenced by the reflection, scattering, and refraction of clouds. H_0 can be obtained from meteorological observation reports or the air-mass lifting condensation level (LCL) (Wang et al., 2017).

To obtain the height of the cloud base of a low cloud, i.e., the LCL of the atmosphere, the following equation can be used (Yang et al., 1982; Wang et al., 2017):

$$H_0 \in P_{LCL} \approx 6.11 \times 10^2 \times \left(\frac{0.622 + 0.622\frac{e_s}{p-e_s}}{0.622\frac{e_s}{p-e_s}}\right) \quad (5)$$

where e_s represents saturated water vapor pressure. The atmospheric low cloud base height is represented by the air pressure (p). When the air pressure (p) of the air mass reaches the saturated water vapor pressure (e_s), but has not yet caused a raindrop to fall, there would be a layer of high water content in the atmosphere (Wang et al., 2017). Such areas of high water content in the atmosphere would be considered the influential atmospheric cloud systems. H is generally consistent with the actual observed low cloud height (H_0).

2.2.5 Contribution of micro scale condensation meteorological conditions to O_3 growth

It is known that NOx/VOCs sources actually dominate the generation of O_3 in the lower troposphere in large cities (Tang et al., 2006). When the VOCs/NOx ratio is appropriate, the wetting drive of the atmospheric condensation rate can accelerate and catalyze O_3 precursors to form secondary pollution, and the O_3 concentration increases exponentially (Wang et al., 2019):

$$\delta O_3 = \alpha(\chi)^{-\beta} = \xi \quad (6)$$

where χ represents O_3 precursors (NOx or VOCs), $\beta = f_c$ is the condensation function, and $\alpha = 10.0 \times 10^3$.

Day-by-day weather change is one of the important physical processes of the atmosphere. This hysterics of radiant heating under the influence of post-sunrise meteorological conditions is related to the delay in O_3 growth. In China, the YRD, the PRD, the NCP, and the Sichuan Basin (SB), the increasing of O_3 concentration in delayed power exponent effecting due to heating on low-layer atmosphere by solar radiation have been observed. As a response to the changing meteorological conditions for the diurnal variation, it is maintained for 3–6 h after sunrise, or even throughout the day, which plays an important role in the increase and decrease of NO_2 and O_3 concentrations. On the basis of multi-station data correlation fitting statistical analysis, the power exponent law is as Eq. 6. The mathematical algorithm of the power exponential growth is a typical description of nonlinear variations. By coefficient of α and β, the power exponent aptly describes the nonlinear variation of the increasing in O_3 concentration due to NO_2 reduction and its regional and seasonal differences (see Table 1). This micro-scale nonlinear contribution is combined with the cloud structure changes discussed in the next section, along with the cross-influence effect of meteorological conditions affected by the solar zenith angle, and the parameterization of PLOM is comprehensively constructed (Wang et al., 2019).

The two coefficients α and β in Eq. 6 give the meteorological characteristics that vary from region to region and from one season to another respectively. The coefficient α represents the contribution efficiency of the law of power exponent for transforming NO_2 into O_3. Study indicated that the magnitude of α for the Yangtze and Pearl River deltas was 10^2–10^3, and that for the inland SB and NCP areas was 10^1. The β denotes magnitude and sign of power, exponent and negative sign means the NO_2 concentration is correlated to the O_3 concentration decline after 3–6 h as a negative power exponent. The magnitude of β was 0.6–1.4, and the majority number is 1.0 (Wang et al., 2019).

In summary, the dimensionless index of standardized O_3 pollution meteorological conditions is expressed as:

TABLE 1 The α and β characteristics of the delayed correlation power exponent in the equation.

	α	β	Delayed time (hours)	Time
Beijing	42.8 × 101	0.9	3	December 2016
Hangzhou	11.0 × 103	1.0	3	September 2016
	19.8 × 102	1.4	6	September 2016
Guangzhou	10.5 × 103	1.7	3	December 2015
	36.4 × 102	1.4	6	December 2015
Chengdu	67.0 × 101	1.0	1	December 2015
	22.6 × 101	0.8	3	December 2015

The stations of Beijing, Hangzhou, Guangzhou and Chengdu are the representative stations of the North China Plain, the Yangtze River Delta, the Pearl River Delta and the Sichuan Basin.

$$PLOM \propto H_0\left(\mu \cos\left(\sin^{-1}\left(\frac{\rho'}{\rho}\right)^{1/2}\right)\right) + \xi \tag{7}$$

3 Results and discussion

3.1 Quantitative description based on parameterization method for severe O_3 pollution event

3.1.1 Observational facts and Parameterization to Link Ozone-pollution with Meteorological index of O_3 pollution in beijing during July 2019

To quantify the influence of meteorological conditions on O_3 pollution from multiple dimensions, typical O_3 pollution events in recent years were analyzed. During the summers of 2017–2020, a rare high-temperature event accompanied by severe O_3 pollution occurred in the NCP. The hottest month in the past 20 years was July 2019, based on the reports of the World Meteorological Organization (WMO) and the National Aeronautics and Space Administration (NASA) (http://www.CRNTT.com). 2019 was also the hottest year in Europe in this century. The temperature in France soared to 37.8°C and a new high-temperature record was set in Britain.

The Beijing Meteorological Observatory issued a yellow high-temperature warning on the afternoon of July 1. The temperature in Beijing continued to rise in July, with the daily maximum temperature going above 35–37°C for many days, and the maximum temperature hovering close to 40°C, with strong ultraviolet intensity and a sharp increase in O_3 concentration.

Figure 3 shows the hourly variations in the PLOM index calculated using the parameterization method in Eq. 7, as well as the temperature, O_3 concentration, and NO_2 concentration. As shown, high temperature and high O_3 pollution occurred frequently in Beijing in July 2019. Temperatures above 35°C and O_3 concentrations above 220 μg m^{-3} were observed in the periods shown in the yellow box of Figure 3. The peak values of temperature (above 37°C) and O_3 concentration (266 and 245 μg m^{-3}) were recorded on July 4 and 21. Moreover, the temperature had a significant diurnal variation synchronized with the O_3 concentration. It is notable that the PLOM index can describe the diurnal variation characteristics consistent with the O_3 concentration for typical severe O_3 pollution cases in Beijing. Figure 3 also shows that the concentrations of NO_2 and O_3 changed in an inverse manner. This indicates that increases in O_3 concentration can be captured under the meteorological conditions of the micro-scale condensation (f_c) described by the PLOM index (see Eq. 7) (Wang et al., 2019). This is an alternative superimposed contribution to the O_3 concentration due to the impact of micro-scale meteorological conditions.

3.1.2 Ability of Parameterization to Link Ozone-pollution with Meteorological index to express seasonal and regional impact of O_3 pollution in China

Figure 4A shows the correlation between the O_3 concentration and PLOM index in Beijing from July 1 to 31, 2019. For two consecutive summers in 2019 and 2020, Beijing suffered from a severe heat wave. Under the high temperature and high humidity "sauna" weather conditions, severe O_3 pollution was encountered in Beijing. Figure 4 indicates that the PLOM index has the important ability to present the O_3 pollution. The PLOM index also has consistent and good expressive ability for O_3 pollution in different years, seasons, and regions. The O_3 concentration positively correlated with the PLOM index; the correlation confirmation coefficients (R^2) were 0.42, 0.53, 0.62, and 0.53 for Beijing for July 2019 and 2020, Hangzhou for September 2015, and Guangzhou for July 2019, respectively, and the significance levels (p) were less than 0.01. Therefore, the PLOM index has important expressive ability to diagnose the influence of meteorological conditions on the change of troposphere O_3 pollution in three representative O_3 pollution areas in China, and the physical mechanisms established by the index are discussed below.

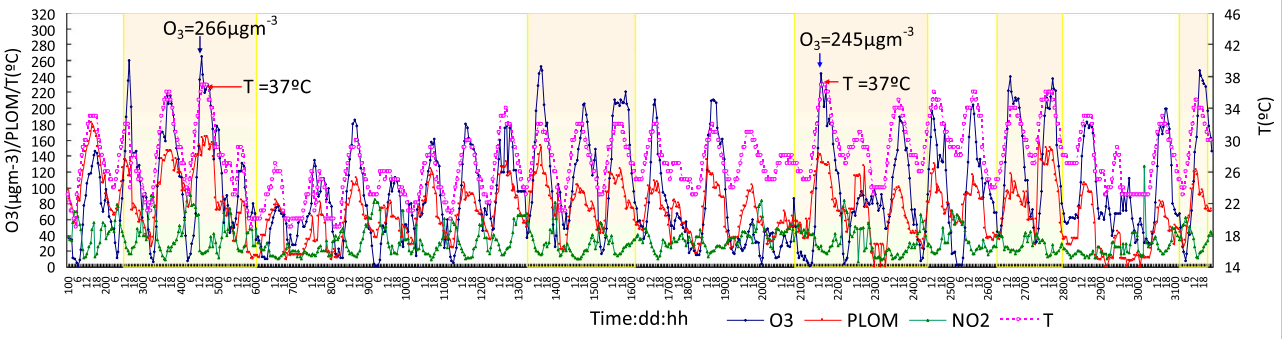

FIGURE 3
Hourly series of PLOM index, temperature, O_3 and NO_2 concentrations from 1 to 31 July, 2019.

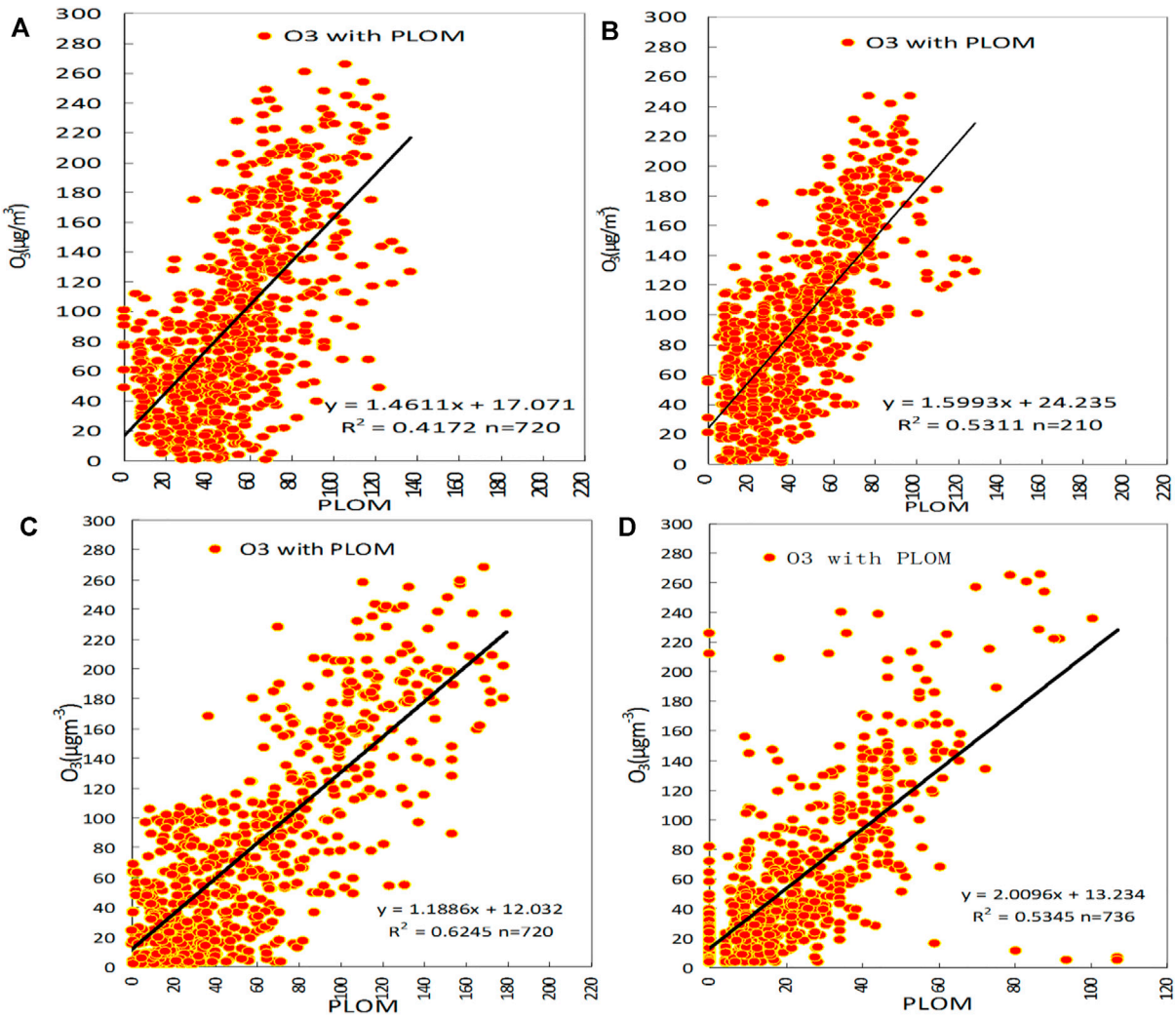

FIGURE 4
(A): Correlation analysis between O_3 concentration and PLOM index from 1 to 31 July, 2019 in Beijing, **(B)**: from 1 to 31 July, 2020 in Beijing, **(C)**: from 1 to 30 September, 2015 in Hangzhou and **(D)**: from 1 to 31 July, 2019 in Guangzhou.

3.2 Contribution of cloud scattering to O_3 under the solar zenith angle changes—driving mechanism based on daily weather condition changes

3.2.1 Cloud scattering effects of different cloud-layer density changes on increase in O_3 concentration

As shown in Figure 2, the zenith angle (Θ_z) is the angle between the sun's incident light and the straight line perpendicular to the ground. Γ_Θ is the impact on O_3 concentration due to the effect of the cloud structure on the reflection, refraction, and scattering of sunlight under different zenith angles under a particular meteorological condition. This depends on the reflection angle (Θ_r) due to the changes in the atmospheric vertical structure, including changes in air pressure (P), temperature (T), and RH distribution with variation in density between the air masses.

From the scattering angle of Eq. 3, the influence of meteorological parameters on the scattering at a certain solar altitude angle can be obtained. The difference in meteorological attributes (temperature (T), pressure (P), water vapor mixing ratio (w)) above and below the cloud is the key to the scattering/reflection and refraction effect of sunlight, which has an effect on the O_3 concentration. At the below-cloud level, solar radiation is refracted through the cloud, and the radiation intensity decreases, whereas scattering and reflection in the above-cloud level increase the solar radiation intensity (irradiance). The change in radiation intensity not only increases or decreases the tropospheric O_3 concentration but also has an important feedback effect, because sunlight reflection will change the densities of the upper and lower levels again. According to Eq. 3, the scattering, reflection, and refraction angles of sunlight entering the atmosphere can be distorted again, and the scattering effect and radiation intensity can be further changed to re-influence the cyclic feedback effect. The parameterization method reveals the impact of meteorological conditions on solar illumination and describes the quantitative influence on the re-contribution to O_3 distribution by connecting the atmospheric attributes (T, P, HR, and ρ) in and above the cloud.

The scattering angle can be calculated using Eq. 3; for the convenience of comparison, the lower layer is assumed to have a 925 hPa height. When the cloud height corresponds to the specified isobaric surface height of 850 (1,500 m) and 700 hPa (3,000 m), the changes in the scattering and reflection angle of solar radiation caused by the change in vertical density (ρ'/ρ) between the upper and lower clouds can be calculated.

Figure 5 indicates the change in scattering angle of solar radiation due to the vertical density difference (ρ'/ρ) between the upper and lower clouds with a cloud height of 1,500 and 3,000 m calculated using Eq. 3. The atmospheric density difference above and below clouds has a significant impact on the scattering of solar radiation. When the density difference changes from 0.6 to 1, the scattering angle changes from 45° to 90°.

There is no difference in density between the cloud and above-cloud level, i.e., ρ'/ρ = 1, which indicates that the cloud has a similar "mirror" reflection effect, the maximum scattering angle is 90°, and the positive contribution to the increase in O_3 concentration is zero. The density ratio (ρ'/ρ) decreases with an increase in the lower atmospheric density. When the density ratio is halved, the reflection angle decreases to 45°, and the contribution can reach the maximum. As shown in Figures 5A,B, the smaller the reflection angle, the greater the positive contribution to the increase in O_3 concentration. This situation just corresponds to the dry and clean meteorological conditions when cold air is inserted into the lower atmosphere. Once the cloud structure changes and the density above and below the cloud changes, the initial cloud reflection changes the solar radiation intensity, as well as enhances radiation above the cloud and increases the O_3 concentration. Changes in a cloud environment and meteorological conditions lead to cooling below the cloud, and ρ'/ρ further decreases (Figure 5A). Based on Eq. 4, the cosine effect will provide feedback and the cloud effect will increase the cloud reflection (Γ_Θ) contribution again, further aggravating the increment in O_3 concentration. Cloud height has an obvious impact on the density difference above and below the cloud. Below 1,500 m, the density difference is typically −0.9–1 and the scattering angle is −85–70°. When the cloud height is 3,000 m, the density difference is −0.7–0.9 and the scattering angle is −70–58°. A change in illuminance depends on the density difference of reflective clouds. A smaller reflection angle corresponds to a greater contribution to the increase in sky brightness and a greater positive contribution to an increase in O_3 concentration. It is also associated with the height of scattering and reflecting clouds; when the cloud is higher, the reflection angle is smaller, and the illumination increases. On the contrary, when the cloud is lower, the reflection angle is larger, and the illumination decreases.

As mentioned above in the Section 2.2.3, when considering the density difference above and below clouds, reflection from fogs and clouds or at any surface of sufficient size (greater than wave-length, dimensions) between masses of air at the same pressure but of unequal density, namely variers from the angle of the zenith (Θ_Z) to the reflection angle with clouds. The contribution of O_3 of reflection effect due to reflection angle (Θ_r) gives as (Humphreys, 1940; Tverski, 1954):

$$\Gamma_\Theta = \Theta_z = \Theta_y \sin^{-1}\left(\frac{\rho'}{\rho}\right)^{1/2} \text{ considering the density difference above and below clouds} \quad (8)$$

Based on Eq. 8, the cosine effect will provide feedback and the cloud effect will increase the cloud reflection (Γ_Θ) contribution again, further aggravating the increment in O_3 concentration. Including the cloud height has an obvious impact on the density difference above and below the cloud. The feedback mechanism is as follows: during the initial phase, cloud reflection can increase solar radiation intensity above the cloud layer, causing O_3 concentration to increase. It also causes cooling below the clouds. So that it is

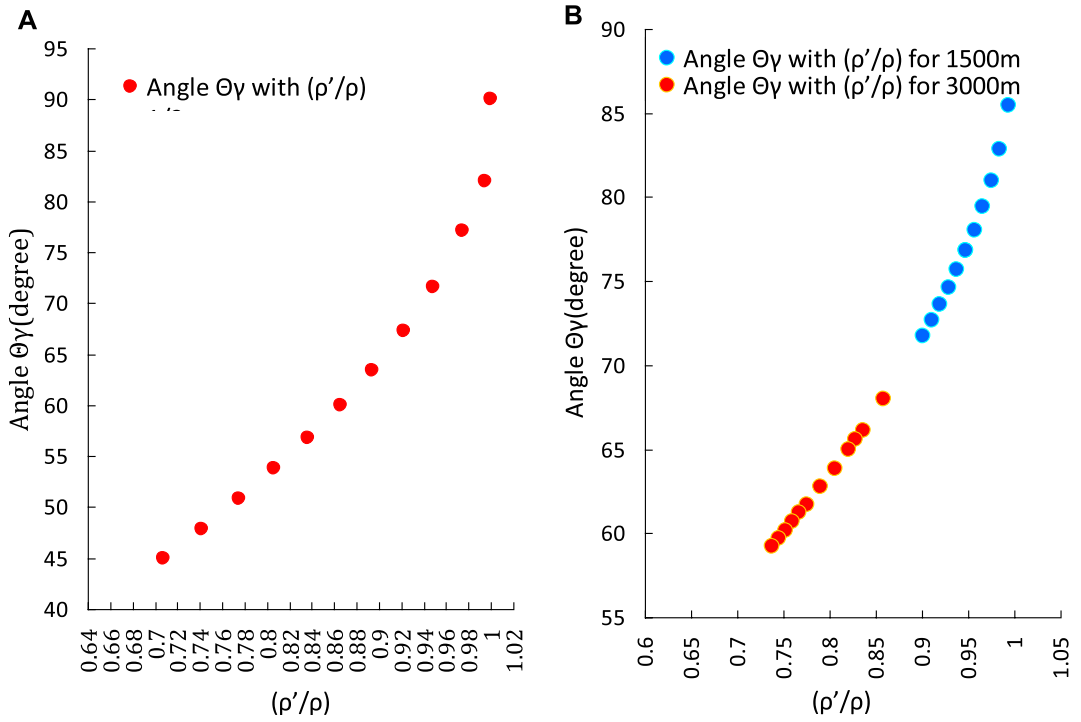

FIGURE 5
(A): The changes of sunlight reflection angle varies with vertical density difference (ρ'/ρ) between above and below of cloud layer, **(B)**: The changes of sunlight reflection angle varies with the vertical density difference (ρ'/ρ) in above and below cloud with the heights of the clouds for 1,500 m and 3,000 m respectively.

further reduced by Eq. 8, resulting (ρ'/ρ)to be increased and the angle of reflection getting increasing (Figure 5A). That is based on Eq. 8, the cosine effect will provide feedback that will again increase the contribution of cloud reflection through (Γ_{Θ}), further exacerbating the increase in O_3 concentration. So, the Eq. 8, as the first term in the PLOM index, describes the direct and feedback contribution of the scattering angle parameter. The second term in the PLOM index, describes contribution of micro scale condensation meteorological conditions to O_3 growth (Wang et al., 2022).

In conclusion, these results show that when the cloud structure changes, the densities of the upper and lower levels change, the solar radiation intensity changes, the radiation above the cloud increases, and the O_3 concentration increases. At the same time, cloud reflection has a dual effect, which will provide feedback and aggravate the increment in O_3 concentration again. The direct and feedback contributions of scattering angle parameters are comprehensively presented in the PLOM index.

3.2.2 Typical cases for contribution of cloud height, cloud scattering, and precursor wetting to increase in O_3 concentrations

Figure 6 shows a typical case of O_3 pollution mentioned above. The variations in various parameters based on the periodic change in the solar zenith angle during the typical peak period of O_3 concentration in Beijing from July 1 to 6, 2019 is given. The rise in cloud height (H0) at daytime and the decrease at night (Figure 6A) was closely linked to the diurnal variation in the solar zenith angle. An increase in daytime δO_3 was observed (Figure 6B). This is the diurnal change of cloud height, the O_3 precursor conversion complements the increment of O_3 (δO_3), i.e. satisfies Eq. 6: $\delta O_3 = \alpha\chi^{-\beta}$. As shown in Figure 6B, the peak of the increment in δO3 is as high as 50–60 μg m^{-3}. When the solar zenith angle is at the zenith (indicated by “”), cloud scattering contributes the most to the increment in O_3 concentration (Figure 6C).

Combined with the impacts of the multi-sensitive meteorological factors discussed herein, the observed O_3 concentration finally increased. The peak value of O_3 concentration was 266 μg m^{-3}, which appeared at 13:00 on July 4. The increment in O_3 concentration can be extended from the zenith angle peak in the evening. The characteristics of the contribution to the increase in O_3 concentration by the influences of precursors and cloud scattering are shown in Figure 6.

Figures 7A,B show the time series of cloud height (H_0) and the contribution of precursor wetting process to O_3 ($\delta O_3 = \alpha\chi^{-\beta}$), respectively during the period of 7–12 February, 2020 in Beijing. Figures 7C,D) show the correlation analysis of

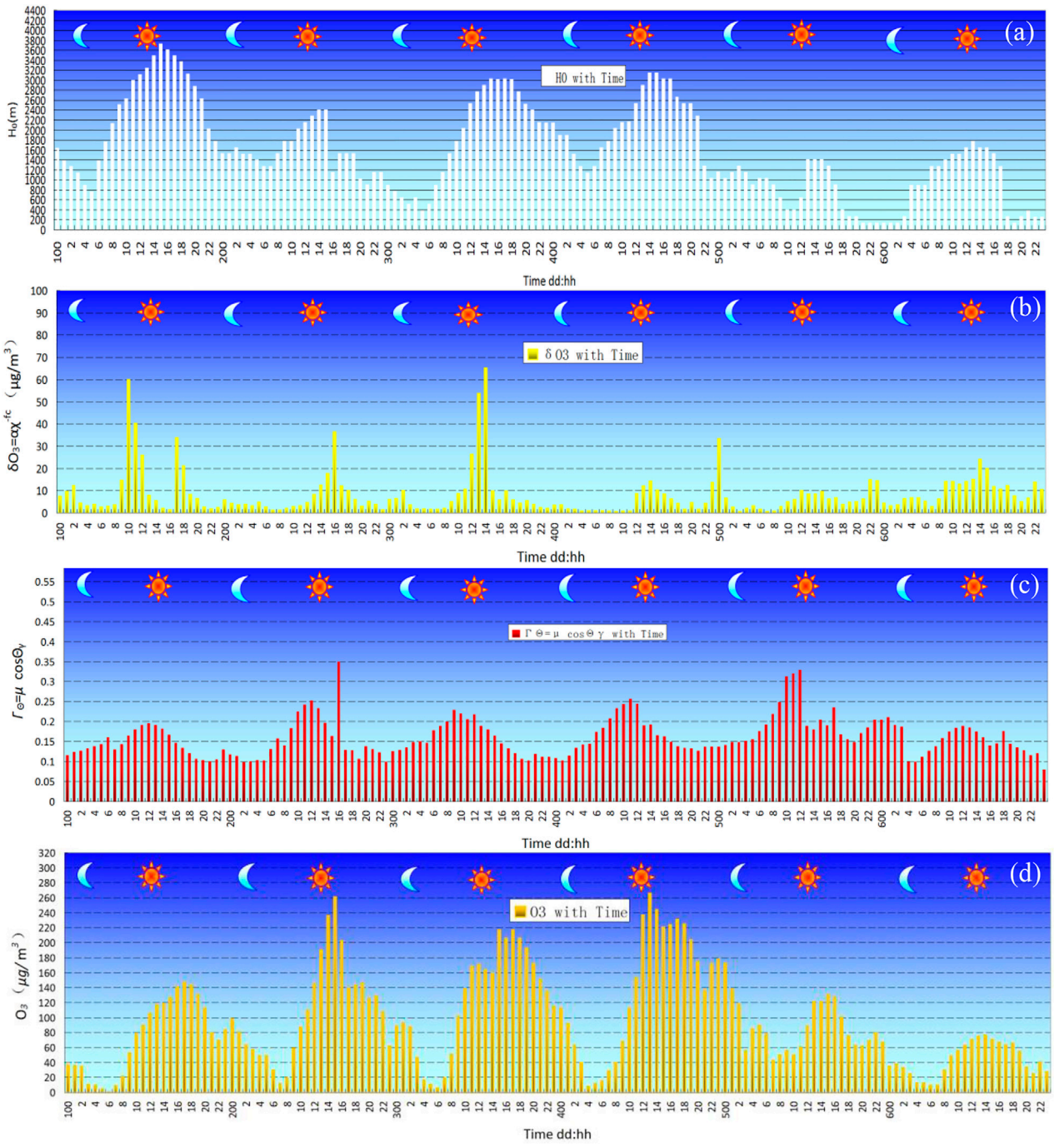

FIGURE 6
(A):Time series of cloud height (H_0), **(B)**: the contribution of precursor wetting process to O_3, **(C)**: the contribution of cloud scattering on O_3 ($\Gamma_\Theta = \mu\cos\Theta_Z$) and **(D)**: the observed O_3 concentration based on the diurnal variation of solar zenith angle during the O_3 peak period in Beijing from 1 to 6 July, 2019.

atmospheric condensation rate (F_c) with O_3 concentration changes for 1 to 6 July 2019 in Beijing corresponding to Figures 6A,B and for 7 to 12 February, 2020 in Beijing (d) corresponding to Figures 7A,B, respectively. It can be seen from the figure that in both summer and winter, it can be observed that with the increase of Fc, the O_3 concentration shows a positive correlation of e-exponential growth, and the correlation confirmation coefficient (R_2) significance level

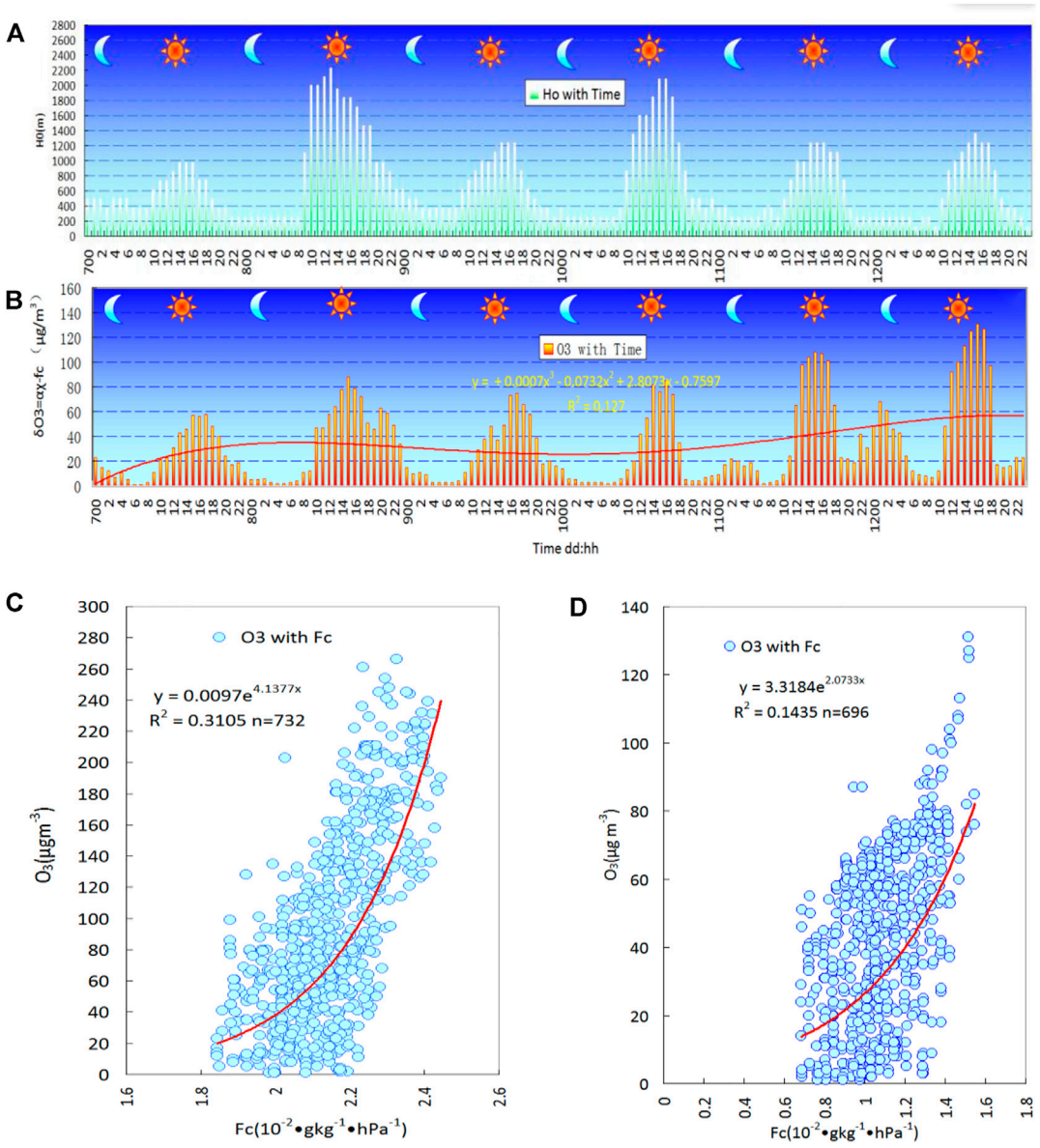

FIGURE 7
During period from February 7 to 12 2020 in Beijing, **(A)**: for hourly the time series of cloud high (H0) in local time, and **(B)**: the time series of precursor wetting process of O_3 in local time. **(C)**: Correlation analysis of Fc with O_3 for 1 to 6 July 2019 for Beijing, corresponding to Figure 6D and **(D)**: 7 to 12 February, 2020 for Beijing, corresponding to Figure 7B.

exceeds 0.001. This suggests that the increase in condensation rate (F_c) is conducive to accelerating and catalyzing the formation of an increase in O_3 concentration.

In summary, it can be seen that the influence of meteorological conditions on the increase in O_3 concentration can aggravate O_3 pollution. The above evidence of the value-added effect of changes in high-resolution meteorological elements on O_3 concentration shows that although the existing understanding based on the chemical mechanism of O_3 formation is based on an approximation of an incomplete knowledge of photochemistry, the increase in O_3 concentration can be extended from the zenith angle peak described in PLOM, which means that wavelength-dependent photochemistry is linked to the influence of clouds on optical characteristics, and the effects of cloud height (the height of the pollution mixed layer) are also included in the design of PLOM. The increase in condensation rate (F_c) in the air is also conducive to accelerating and catalyzing the formation of an increase in O_3 concentration. Therefore, it is practical and necessary for this study, to establish quantitative PLOM parameters, focusing on

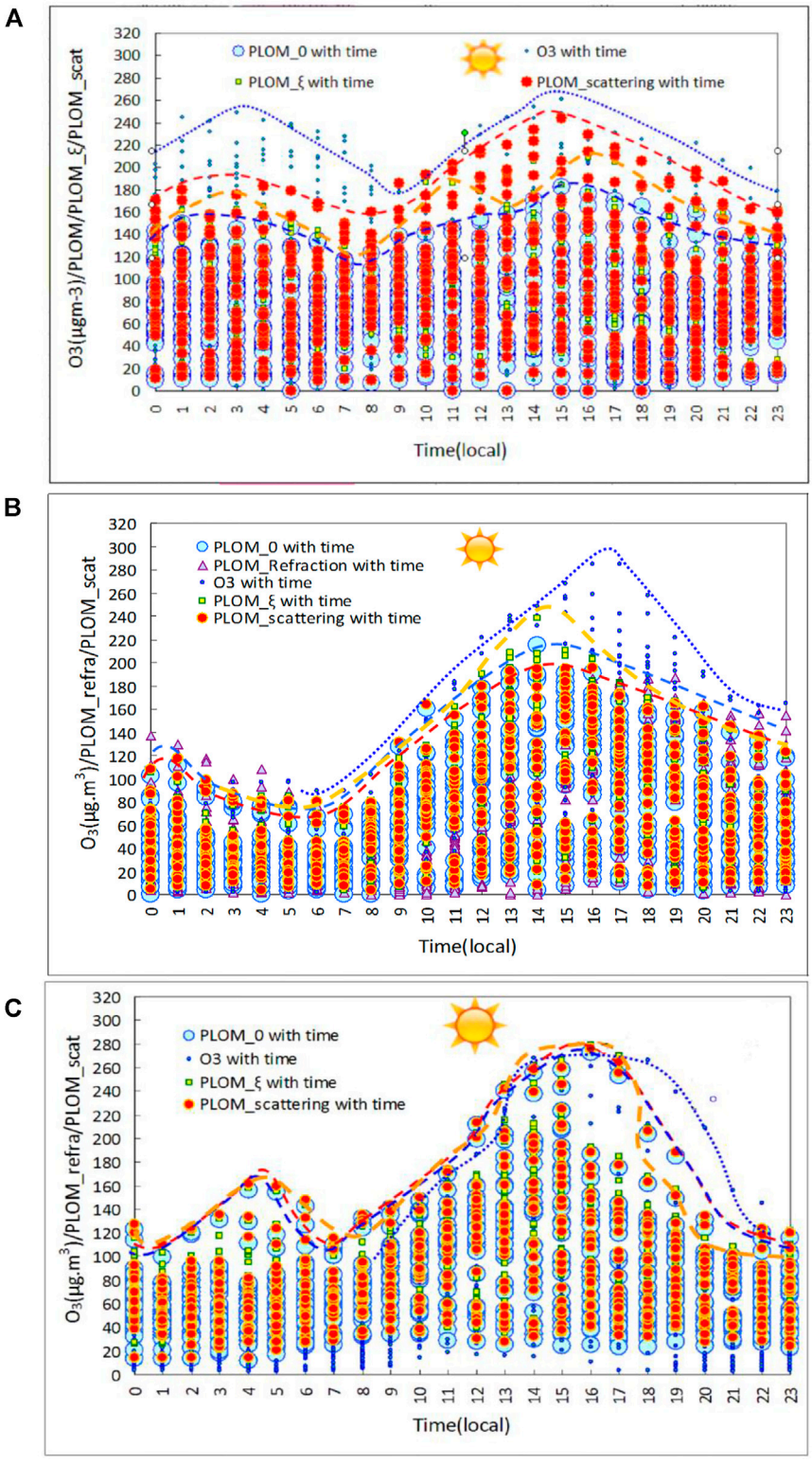

FIGURE8
(A): Time series of PLOM_0 (blue dotted line), PLOM with scattering effect (red dashed line), PLOM_$\xi(\delta O_3 = \alpha(NO_2)^{-fc})$with contributed by O_3 precursors (yellow dashed line), as well as O_3 concentration (blue thin dotted line) in Beijing from 1 to 31 July, 2019. **(B)**: Similar to **(A)**, but in Hangzhou from 1 to 30 September, 2015. **(C)**: in Guangzhou from 1 to 31 July, 2019. The red fill circle and red dashed line represent the distributions of PLOM and the outline of its maximum values, includes additional cloud scattering effects at daytime respectively. The filled circle with relative larger

(*Continued*)

FIGURE8 (Continued)
light blue fill and blue dashed line represent the values of PLOM_0 and outline of its maximum values, respectively. Small rectangular icons with green boxes and yellow fills, along with yellow dotted lines, represent the distributions of PLOM_ξ ($\delta O_3 = \alpha(NO_2)^{-fc}$)and the outline of its maximum values, respectively. The blue small circle and thin dotted line represent the observed values of O_3 and outline of its maximum values of O_3, respectively. The triangle describes the contributions of sunlight refraction to O_3 weakening.

and supplementing the additional effect of meteorological conditions on increasing more O_3 values.

3.2.3 Diurnal variation characteristics of O_3 increases due to cloud scattering

In order to consider the PLOM parametric description based on the effect of solar altitude angle diurnal changes on O_3 in the establishment of the PLOM index, consider the contribution of higher atmospheric condensation rate (f_c) to fine particulate matter and O_3 precursors, which is conducive to O_3 growth. This is because the impact of changes in atmospheric condensation rate (f_c) can also cover the indirect contribution of clouds to O_3 growth, including the contribution of diurnal variations in cloud height (height of the mixed layer of pollution) to O_3 growth (see Figures 6, 7). Based on the describing ability of PLOM mentioned above, by using a kind of the daily cycle synthesis profile analysis method (Wang et al., 2019), an analyzing of the different regional differences in the hourly distribution of cloud scattering effects of each parameter in NCP, YRD and PRD during severe O_3 pollution was given as shown in Figure 8.

Figure 8 shows the diurnal cycle synthetic sections of the hourly distribution of the effects of cloud scattering and the hourly distribution of O_3 precursor conversion with O_3 concentration during the severe O_3 pollution period in Beijing from July 1 to 31, 2019 (Figure 8A), in Hangzhou from September 1 to 30, 2015 (Figure 8B), and in Guangzhou from July 1 to 31, 2019 (Figure 8C).

The solar zenith angle has some different effect on the diurnal variation in O_3 concentration in the inland and coastal areas. The solar zenith angle $\Theta_z = 0^\circ$ represents noon (local time). Unlike the near-coastal areas close to Hangzhou and Guangzhou, the diurnal variation in O_3 concentration shows a significant double peak in Beijing, which occurs at 03:00-08:00 (4–9 h before noon) and 14:30 (2.5 h after noon). The O_3 concentration was as high as 250 μg m^{-3} in the morning and 266 μg m^{-3} at 14:00. The peak value of O_3 was observed in the afternoon only in Hangzhou and Guangzhou, at 17:30 and 16:00, respectively, lagging behind noon by 4–5.5 h, 1.5-3 h behind that in the NCP. The contribution of O_3 precursors to the increase in O_3 concentration was 28% in Beijing, and 11% and 13% in Hangzhou and Guangzhou, respectively (Table 2 and Figures. 8A–C). The bimodal distribution of O_3 concentration in the morning and afternoon in Beijing was 10 h ahead of and 4 h behind noon. The Hangzhou and Guangzhou lag was 2.5–4.5 h.

Micrometeorological conditions had a greater influence on the wetting process of O_3 precursors, and the lag period and influence intensity were significantly different between the north and south areas. In addition, the contribution of cloud scattering to the increment in O_3 concentration was 19%, 8%, and 4% in Beijing, Hangzhou, and Guangzhou, respectively (indicated by the red dotted line and red solid circle in Figure 8). The impact intensity in the NCP was more than twice that in the YRD and PRD, and the peak lagged about 2.5–4.5 h behind noon. The loss rate of tropospheric O_3 concentration caused by cloud refraction in Hangzhou was −6%, and the lag time was up to 6 h.

In summary, meteorological conditions, including the scattering and refraction of sunlight by clouds and atmospheric condensation, have an obvious effect on the wetting process of O_3 precursors. They also have a significant impact on the occurrence time and intensity of the tropospheric O_3 concentration peak, which shows that the PLOM index is of great significance in the diagnosis and prediction of the temporal and spatial distribution of severe O_3 pollution.

3.3 Quantitative comparative analysis of application of Parameterization to Link Ozone-pollution with Meteorological index to meteorological conditions and emission reduction during typical severe pollution cases

Zhang et al. (2009; 2018b) proposed a quantitative and objective evaluation method based on the PLAM index for the contribution of meteorological conditions and emission to aerosol pollution. This method can provide an important objective basis for the government to assess and make emission reduction decisions (Zhang et al., 2009; Wang et al., 2018). For aerosol pollution, the objective and quantitative discrimination of the rate of change of the contribution of meteorological conditions is $\lambda = (\alpha_B - \alpha_A)/\alpha_B$. α_B and α_A represent the slope of the fitting curve between the PLAM index and aerosol pollution concentration (e.g., $PM_{2.5}$) during the different periods (B and A), respectively (Zhang et al., 2018b). The PLAM index discrimination principle is also applicable to the PLOM index in this study. Figure 9 shows the comparison between PLOM during severe O_3 pollution in 2019 and the same period in 2018. For severe O_3 pollution in 2019, compared with meteorological conditions in the same periods in 2018, the discrimination is $\lambda = (\alpha_{2018} - \alpha_{2019})/\alpha_{2018}$.

TABLE 2 Effects of Θ_z on tropospheric ozone concentrations based on cloud scattering, refraction, and ozone precursors.

City	Peak time of O_3	Hours ahead of/ behind Θ_z = 0	Contribution rate of O_3 affected by ξ (%)	Hours behind Θ_z = 0° due to ξ influences	Contribution rate of O_3 affected by cloud scattering (%)	Hours behind Θ_z = 0° due to cloud scattering influences	Contribution rate of O_3 affected by cloud reflections
BJ	01:00/14:30	10/2.5	28	4.0	19	2.5	—
HZ	17:30	/5.5	11	2.5	8	2.5	−6%
GZ	16:30	/4.5	13	4.5	4	4.5	—

TABLE 3 Comparison of contribution of meteorological conditions in 2019 and 2018.

Year	Contrast studies	α	Average O_3 concentration
2018	Observation in 2018	2.16	90.8 μg m^{-3}
2019	Observation in 2019	1.46	95.5 μg m^{-3}
2019	If no emission reduction in 2019	—	119.9 μg m^{-3}
2019 to 2018	λ = (α2018 - α2019)/α2018	0.32	—

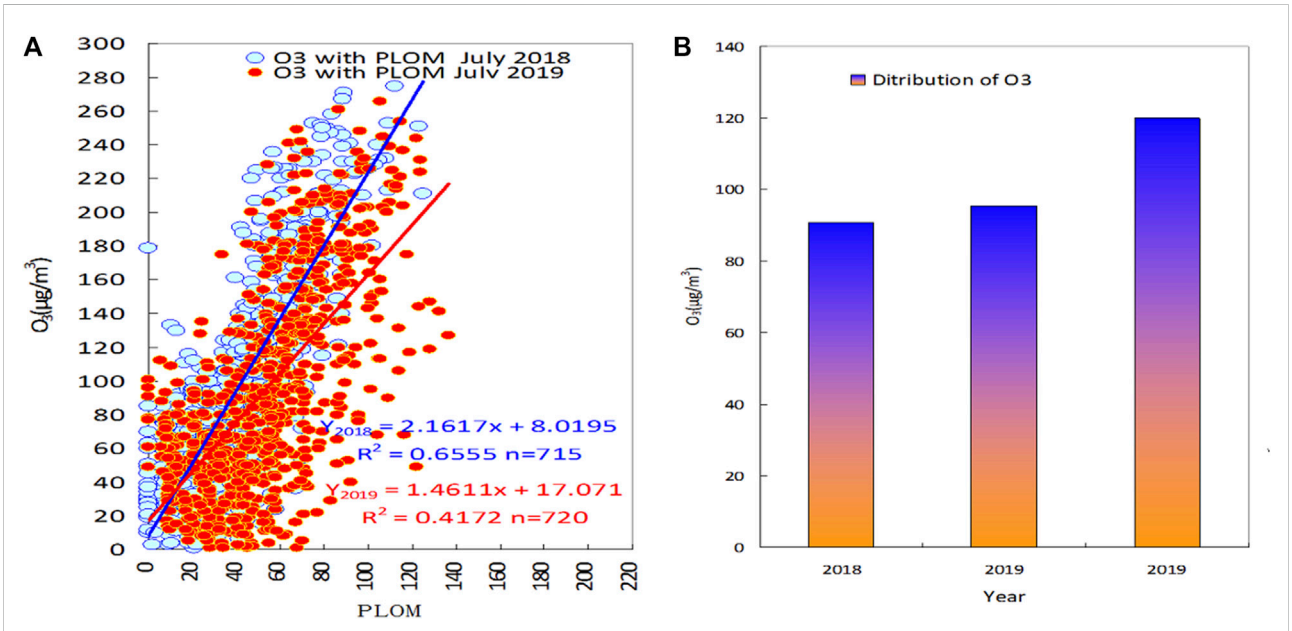

FIGURE 9
(A): Comparison analyses of contribution of meteorological conditions between typical severe O_3 pollution in 2019 and 2018; **(B)**: The observational O_3 concentration in 2018 and 2019 (left and medium), and regardless of emission reductions, O_3 concentrations in 2019 (right).

Compared with the observed change in O_3 concentration in 2018, the O_3 concentration was expected to increase by 32% due to unfavorable meteorological conditions in 2019; however, the actual observation only increased by −4.9%, indicating that the emission reductions still contributed to a reduction in O_3 concentration by −27.1%.

The variation rate of unfavorable meteorological conditions for O_3 concentration was 32% in 2019; under the same meteorological conditions, the average value of O_3 concentration can be the higher value of 119.9 μg m^{-3} in 2019 (see Figure 9B (right)). The monthly average observed value of O_3 concentration was 95.5 μg m^{-3}, a decrease of 25–30%, which

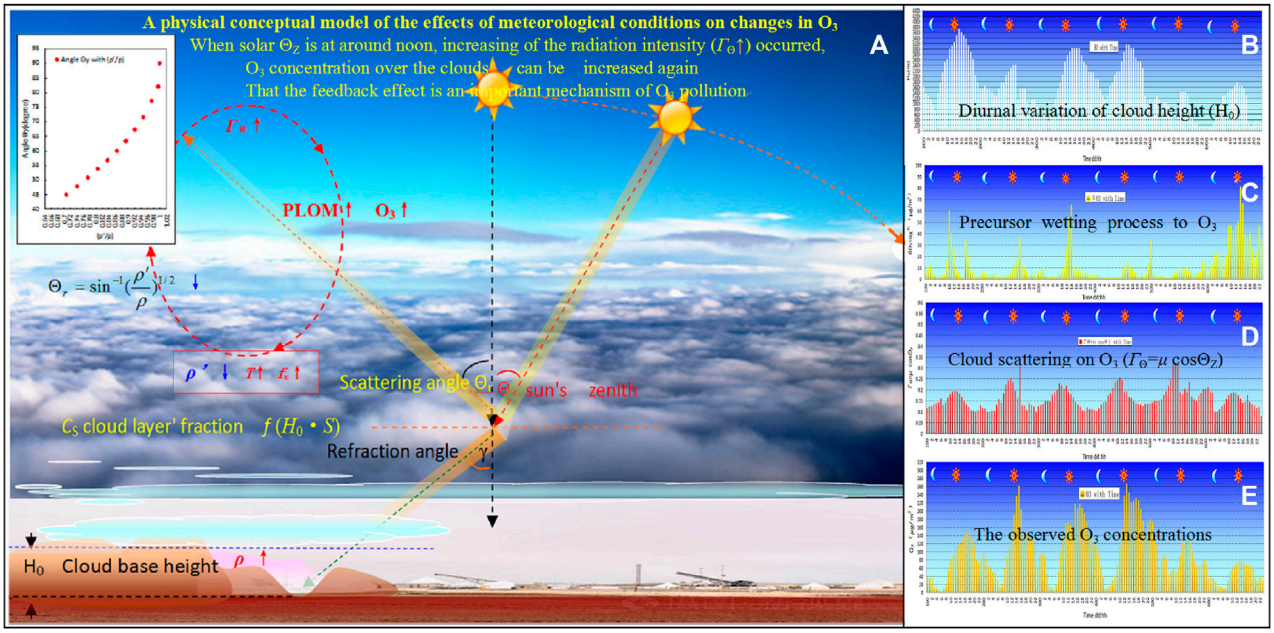

FIGURE 10
Conceptual diagram of the effect of meteorological conditions on ozone pollution.

indicates the importance of the contribution of emission reduction measures (Table 3).

4 Conclusion

The relationship between tropospheric O_3 pollution and meteorological conditions in the main sensitive areas in China was analyzed and demonstrated, by using the atmospheric component data for Beijing, Hangzhou, and Guangzhou. Based on quantitative description theories of cloud scattering, cloud height, cloud volume, and cloud structure changes, as well as feedback effects caused by water vapor condensation, a parametric PLOM index model for the analysis and diagnosis of O_3 pollution events was established. Clouds are representative parameters that affect the multi-parametric variations of meteorological conditions, and it covers both direct and indirect effects. The design of the PLOM index introduces changes in cloud structure, so that the effects of cloud shape, cloud height, solar zenith angle, cloud scattering, etc. Are included. And a closer relationship with water vapor condensation related to the transformation of O_3 precursors, leading to the temporal and spatial variations in the tropospheric O_3 concentration is included also. The comprehensive structure of the index puts forward a diagnostic quantitative model and physical concept for the influence of meteorological conditions on the variation in O_3 concentration, as shown in the Figure 10. The major findings were as follows:

(1) Under conditions with influence clouds, the incremental values of O_3 concentrations exhibit a process of cyclic feedback and reinforcement. When the difference in the cloud scattering angle (Θ_r) above the cloud and in the cloud is smaller (e.g., 0–45°), the solar radiation (luminance) increases, and the PLOM index and O_3 concentration increase again.
(2) Under the condition of having influence clouds, feedback effect is an important mechanism of O_3 pollution due to density decreases (increases) in the upper (lower) level over (below) the cloud, which is associated with solar radiation intensity over the clouds.
(3) The PLOM index diagnosis of typical severe O_3 pollution cases shows the effect of cloud scattering significantly contributes to the increase in tropospheric O_3 concentration. The contribution rates were 19%, 8%, and 4% in Beijing, Hangzhou, and Guangzhou, respectively. The significant regional difference in precursor wetting triggered by micrometeorological impacts on the increase in O_3 concentration indicates that it has a more obvious impact inland.
(4) The PLOM index has universality and expressive ability. The correlation analysis of four typical cases of severe O_3 pollution in Beijing (0.42), Hangzhou (0.53), and Guangzhou (0.62) revealed that the PLOM index positively correlated with the change in O_3 concentration.
(5) The PLOM index established in this study can provide a quantitative and objective basis, and decision-making guidance, for the Meteorological Forecasting Center's

consultation to accurately assess the relative contribution of emission reduction and meteorological conditions.

Data availability statement

The original contributions presented in the study are included in the article/Supplementary Material, furtherinquiries can be directed to the corresponding author.

Author contributions

JW, DW, and YY designed the research and led the overall scientific questions. YY, DW, XJ, WJ, and YW carried out data processing and analysis. WJ and XJ helped with data processing. DW wrote the first draft of the manuscript and then JW revised the manuscript. All authors read and approved the final version.

Funding

This study is supported jointly by the Major National Natural Science Foundation of China Project (42090031), the National Natural Science Foundation of China Project (U19A2044), National Natural Science Foundation of China (41675121), the Basic Scientific Research Progress of the Chinese Academy of Meteorological Sciences (2016Z001), the National Key Project of Basic Research (2014CB441201, 453172).

Acknowledgments

The authors would like to thank Academician Zhang X.Y. for his valuable suggestions and comments.

Conflict of interest

The authors declare that the research was conducted in the absence of any commercial or financial relationships that could be construed as a potential conflict of interest.

Publisher's note

References

Ackerman, A. S., Kirkpatrick, M. P., Stevens, D. E., and Toon, O. B. (2004). The Impact of humidity above stratiform clouds on indirect aerosol climate forcing. *Nature* 21, 1014–1017. doi:10.1038/nature03174

Bohn, B., Corlett, G. K., Gillmann, M., Sanghavi, S., Stange, G., Tensing, E., et al. (2008). Photolysis frequency measurement techniques: Results of a comparison within the ACCENT project. *Atmos. Chem. Phys.* 8, 5373–5391. doi:10.5194/acp-8-5373-2008

Bokoye, A. I., Royer, A., O'Neil, N. T., Cliche, P., Fedosejevs, G., Teillet, P., et al. (2001). Characterization of atmospheric aerosols across Canada from a ground-based sunphotometer network: Aerocan. *Atmosphere-Ocean* 39 (4), 429–456. doi:10.1080/07055900.2001.9649687

Dunya, A., Philippe, K., Alain, S., Bock, O., Irbah, A., Bekki, S., et al. (2017). Enhanced MODIS atmospheric total water vapour content trends in response to arctic amplification. *Atmosphere* 8 (12), 241. doi:10.3390/atmos8120241

Hu, Y. T., Zhao, P., Niu, J. F., Sun, Z., Zhu, L., and Ni, G. (2016). Canopy stomatal uptake of NOX, SO2 and O3 by mature urban plantations based on sap flow measurementflow measurement. *Atmos. Environ. X.* 125, 165–177. doi:10.1016/j.atmosenv.2015.11.019

Humphreys, W. J. (1940). *Physics of the air*. 3rd Ed., 676. Part3:Chaptre1).

Kuo, H. L. (1961). Convection in conditionally unstable Atmosphere. *Tellus* 13, 441–459. doi:10.1111/j.2153-3490.1961.tb00107.x

Kuo, H. L. (1974). Further studies of the parameterization of the influence of cumulus convection on large-scale flow. *J. Atmos. Sci.* 31, 1232–1240. doi:10.1175/1520-0469(1974)031<1232:fsotpo>2.0.co;2

Kuo, H. L. (1965). On formation and intensification of tropical cyclones through latent heat release by cumulus convection. *J. Atmos. Sci.* 22, 40–63. doi:10.1175/1520-0469(1965)022<0040:ofaiot>2.0.co;2

Li, J., Chen, H. B., Li, Z. Q., Wang, P., Cribb, M., and Fan, X. (2015). Low-level temperature inversions and their effect on aerosol condensation nuclei concentrations under different large-scale synoptic circulations. *Adv. Atmos. Sci.* 32 (7), 898–908. doi:10.1007/s00376-014-4150-z

Li, Y., Wang, W., Wang, J. Z., Zhang, X., Lin, W., and Yang, Y. (2011). Impact of air pollution control measures and weather conditions on asthma during the 2008 Summer Olympic Games in Beijing. *Int. J. Biometeorol.* 55, 547–554. doi:10.1007/s00484-010-0373-6

Liu, L. K., Zhang, X. Y., Zhong, J. T., Wang, J., and Yang, Y. (2019). The 'two-way feedback mechanism' between unfavorable meteorological conditions and cumulative PM2.5 mass existing in polluted areas south of Beijing. *Atmos. Environ. X.* 208, 1–9. doi:10.1016/j.atmosenv.2019.02.050

Madronich, S., and Flocke, S. (1999). *The role of solar radiation in atmospheric chemistry*. Berlin, Heidelberg: The Handbook of Environmental Chemistry.

Platnick, S., Durkee, P. A., Nielsen, K., Taylor, J. P., Tsay, S. C., King, M. D., et al. (2000). The role of background cloud microphysics in the radiative formation of ship tracks. *J. Atmos. Sci.* 57, 2607–2624. doi:10.1175/1520-0469(2000)057<2607:trobcm>2.0.co;2

Qu, H., and Chen, S. B. (2002). The application prospect of the medium resolution imaging spectrometer (MODIS) data in geosciences. *World Geol.* 21, 176–180.

Sheng, Z. Z., Che, H. Z., Chen, Q., Xia, X., Liu, D., Wang, Z., et al. (2019). Aerosol vertical distribution and optical properties of different pollution events in Beijing in autumn 2017. *Atmos. Res.* 215, 193–207. doi:10.1016/j.atmosres.2018.08.029

Tang, X. Y., Zhang, Y. H., and Shao, M. (2006). *Atmospheric environmental chemistry*. China: Higher Education Press.

Textor, C., Schulz, M., Guibert, S., Kinne, S., Balkanski, Y., Bauer, S., et al. (2006). Analysis and quantification of the diversities of aerosol life cycles within AeroCom. *Atmos. Chem. Phys.* 6, 1777–1813. doi:10.5194/acp-6-1777-2006

Tverski, P. H. (1954). *Introduction to meteorology*. Russian: Hydrometeorology Press.

Wang, D. Y., Wang, J. Z., Yang, Y. Q., Liangke, L., Junting, Z., and Yaqiang, W. (2021). Formation mechanism of heavy haze-fog associated with the interactions

between different scales of atmospheric processes in China. *Atmos. Pollut. Res.* 12, 101085. doi:10.1016/j.apr.2021.101085

Wang, H. L., and McFarquhar, G. M. (2008). Modeling aerosol effects on shallow cumulus convection under various meteorological conditions observed over the Indian Ocean and implications for development of mass-flux parameterizations for climate models. *J. Geophys. Res.* 113 (D20), D20201. doi:10.1029/2008jd009914

Wang, H., Lyu, X. P., Guo, H., Wang, Y., Zou, S., Ling, Z., et al. (2018). Ozone pollution around a coastal region of South China Sea:interaction between marine and continental air. *Atmos. Chem. Phys.* 18, 4277–4295. doi:10.5194/acp-18-4277-2018

Wang, J. Z., Gong, S., Zhang, X. Y., Yang, Y. Q., Hou, Q., Zhou, C. H., et al. (2012). A parameterized method for air-quality diagnosis and its applications. *Adv. Meteorology* 238589, 1–10. doi:10.1155/2012/238589

Wang, J. Z., Yang, Y. Q., Jiang, X. F., Wang, D. Y., Zhong, J. T., and Wang, Y. Q. (2022). Observational study of the PM2.5 and O3 superposition-composite pollution event during spring 2020 in Beijing associated with the water vapor conveyor belt in the northern hemisphere. *Atmos. Environ. X.* 272, 118966. doi:10.1016/j.atmosenv.2022.118966

Wang, J. Z., Yang, Y. Q., Zhang, X. Y., Liu, H., Che, H., Shen, X., et al. (2017). On the influence of atmospheric super-saturation layer on China's heavy haze-fog events. *Atmos. Environ. X.* 171, 261–271. doi:10.1016/j.atmosenv.2017.10.034

Wang, J. Z., Yang, Y. Q., Zhang, Y. M., Niu, T., Jiang, X., Wang, Y., et al. (2019). Influence of meteorological conditions on explosive increase in O3 concentration in troposphere. *Sci. Total Environ.* 652, 1228–1241. doi:10.1016/j.scitotenv.2018.10.228

Wang, S. L., and Chai, F. H. (2002). A study on O3 pollutions in Beijing, 2002. *Geo-Science (in Chin.* 22 (3), 360–364.

Webb, A. R., and Steven, M. D. (1986). Daily totals of solar UVB radiation estimated from routine meteorological measurements. *J. Climatol.* 6, 405–411. doi:10.1002/joc.3370060406

Yang, D. S., Liu, Y. B., and Liu, S. K. (1982). Dynamics of meteorology. 297–359.

Yang, Y. Q., Wang, J. Z., Hou, Q., and Yaqiang, W. (2009). A plam index for Beijing stabilized weather forecast in summer over Beijing. *J. Appl. Meteorol. Sci. (in Chin.* 20, 643–649.

Yang, Y. R., Liu, X. G., Qu, Y. J., An, J. L., Jiang, R., Zhang, Y. H., et al. (2015). Characteristics and formation mechanism of continuous hazes in China: A case study during the autumn of 2014 in the north China plain. *Atmos. Chem. Phys.* 15 (14), 8165–8178. doi:10.5194/acp-15-8165-2015

Zhang, X. Y., Sun, J. Y., Wang, Y. Q., Li, W. J., Zhang, Q., Wang, W. G., et al. (2013). Factors contributing to haze and fog in China (in Chinese). *Chin. Sci. Bull.* 58, 1178–1187.

Zhang, X. Y., Wang, Y. Q., Lin, W. L., Zhang, Y. M., Zhang, X. C., Gong, S., et al. (2009). Changes of atmospheric composition and optical properties over beijing 2008 olympic monitoring Campaign. *Bull. Am. Meteorol. Soc.* 90 (11), 1633–1652. doi:10.1175/2009bams2804.1

Zhang, X. Y., Zhong, J. T., Wang, J. Z., Wang, Y., and Liu, Y. (2018). The interdecadal worsening of weather conditions affecting aerosol pollution in the Beijing area in relation to climate warming. *Atmos. Chem. Phys.* 18, 5991–5999. doi:10.5194/acp-18-5991-2018

Zhang, Y. M., Wang, J. Z., Yang, Y. Q., Li, D., Wang, Y. Q., Che, H., et al. (2018). Contribution distinguish between emission reduction and meteorological conditions to "Blue Sky". *Atmos. Environ. X.* 190, 209–217. doi:10.1016/j.atmosenv.2018.07.015

Zhang, Y. M., Zhang, X. Y., Sun, J. Y., Lin, W. L., Gong, S. L., Shen, X. J., et al. (2011). Characterization of new particle and secondary aerosol formation during summertime in Beijing, China. *Tellus B* 63, 382–394. doi:10.3402/tellusb.v63i3.16221

Zhao, Q., Yao, W., Zhang, C., Wang, X., and Wang, Y. (2019). Study on the influence of fog and haze on solar radiation based on scattering-weakening effect. *Renew. Energy* 134, 178–185. doi:10.1016/j.renene.2018.11.027